7

Laser-Light Scattering Approach to Peptide–Membrane Interaction

Marco M. Domingues and Nuno C. Santos

Abstract

Membrane-active peptides are becoming widely used, mainly due to their high therapeutic potential. Although the therapeutic action is characterized, the mechanisms of interaction are often unclear or controversial. In biophysical studies, non-invasive techniques are overlooked when studying the effect of peptides on membranes. Light scattering techniques, such as dynamic light scattering and static light scattering, can be used as tools to determine whether promotion of membrane aggregation in the presence of peptides and of self-peptide aggregation in solution occurs. More recently, light scattering has been used for evaluating the alteration on membrane surface charge (ζ-potential) promoted by membrane–peptide interactions. The data obtained by these techniques (either by themselves or combined with complementary experimental approaches) therefore yield valuable elucidations of membrane-active peptides' mechanisms of action at the molecular level.

7

Laser-Light Scattering Approach to Peptide–Membrane Interaction

Marco M. Domingues and Nuno C. Santos

Instituto de Medicina Molecular, Faculdade de Medicina, Universidade de Lisboa, Lisboa, Portugal*

7.1. Introduction

The basis of the light-scattering theory was developed by John William Strutt (Lord Rayleigh) in the final decades of the 19th century.[1] In the first half of the 20th century Debye and Gans[2] developed the theory, as

*Institute of Molecular Medicine, School of Medicine, University of Lisbon, Lisbon, Portugal

well as methods based on it. Because of the noninvasive properties of light-scattering-based techniques, they can be useful tools for studying the action of membrane-active peptides. These techniques have been used to determine the weight-average molecular weight (M_w), size (given by the value of the intensity-weighted mean hydrodynamic radius, R_H), and aggregation behavior of peptide in solution, either alone or interacting with more complex systems such as lipid membranes. The most frequently used techniques based on light scattering are the so-called intensity or static light scattering (SLS) and dynamic light scattering (DLS). SLS was first developed by Debye and Zimm in the 1940s for the determination of M_w and intermolecular interactions.[3–5] It is advantageous for studies of proteins or peptide aggregation in solution.[6–8] Peptide aggregation monitored by SLS can yield stoichiometry data by direct relation to the calculated M_w. DLS began to be applied as an analytical tool only in the 1960s, after lasers were developed and used as monochromatic and intense light sources. It is used to measure particle hydrodynamic diameter and size distribution of molecules or supramolecular aggregates.[9–15] Another technique associated with light-scattering phenomena arose later: the ζ-potential determination. The parameter quantifies the charge of the molecule or supramolecular aggregate at its surface, in contact with the aqueous environment. Thus, light-scattering spectroscopy is of potential applicability in membrane-active-peptide work: (1) as DLS and SLS techniques are very sensitive to changes in shape and size, peptide aggregation or peptide-induced aggregation of lipid membranes can be easily detected, and (2) charged peptides interact with charged vesicles, altering the electrophoretic mobility of the resulting supramolecular entities and enabling ζ-potential measurements to be used to study the membrane events involved in the process.

7.2. Static Light Scattering

SLS uses the time-averaged intensity of the sample in a long time scale relative to molecular diffusion (seconds to minutes) instead of fluctuations of the signal because of molecular dynamics in the scattering volume (microsecond time range). This technique enables the determination

of M_w (typically ranging from 1 kDa to 20 MDa) and the second virial coefficient (A_2) through the Zimm method:[4,5]

$$\frac{KC}{R_\theta} = \frac{1}{M_W P(\theta)} + 2A_2C, \tag{7.1}$$

where

$$K = \frac{2\pi^2}{\lambda_0^4 N_A}\left(n_0 \frac{dn}{dC}\right)^2, \tag{7.2}$$

$$R_\theta = \frac{I_A n_0^2}{I_R n_R^2} R_R, \tag{7.3}$$

and

$$P(\theta)^{-1} = \left(1 + \frac{q^2 {R_g}^2}{3}\right). \tag{7.4}$$

In the preceding equations, C is the concentration of the scattering particles, K—the optical constant, A_2—the second virial coefficient, N_A—Avogadro's number, R_θ—the Rayleigh ratio, I_R—the reference scattering intensity (pure toluene and benzene are the more commonly used reference samples), I_A—the residual intensity of the solute (i.e., the scattering intensity of the sample after subtracting the scattering intensity of the solvent), n_0—the solvent refractive index, n_R—the reference refractive index, λ_0—the vacuum wavelength of the incident light, dn/dC the—refractive index increment (relates to how much the refractive index of a solution changes with the concentration of the solute), R_R—the Rayleigh ratio of the reference, $P(\theta)$—the intraparticle structure factor (accounts for the interference of light scattered from different points of the same particle), θ—the angle at which the intensity is being measured relative to the transmitted beam, R_g—the radius of gyration (shape-independent parameter related to the dimension of the scattering particle), and q is the scattering vector:

$$q = \frac{4\pi n_0}{\lambda} \sin\left(\frac{\theta}{2}\right). \tag{7.5}$$

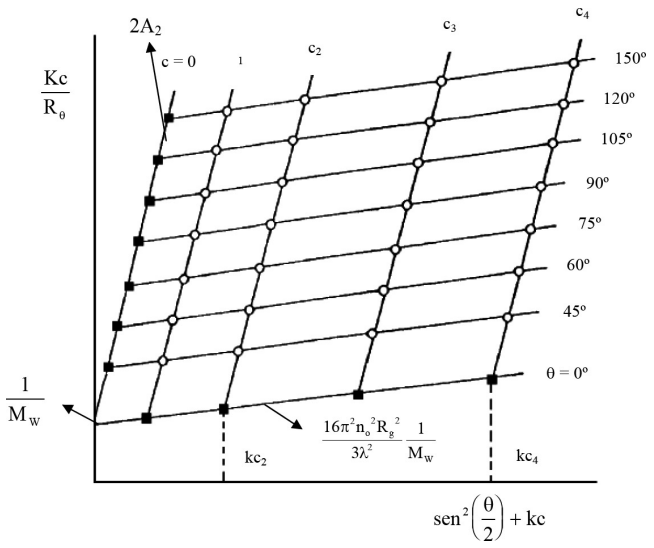

Figure 7.1. Representation of the Zimm plot method and the parameters A_2, M_w and R_g, obtained from the slopes and intercept of the lines obtained from the extrapolations of the experimental data to zero scattering angle and zero concentration.

In the Zimm method (**Fig. 7.1**), M_w is calculated by extrapolation of the scattered intensity both to zero angle (**Eq. 7.6**) and infinite dilution **(Eq. 7.7**). A_2 describes the interparticle interactions: positive values indicate a tendency toward stable scattering particles (monomers) in solution, while negative values reveal a tendency for aggregation (i.e., solute–solute interactions superimpose to solute–solvent interactions). It is calculated by the slope of **Eq. 7.6**.

$$\frac{KC}{R_\theta} = \frac{1}{M_W} + 2A_2C, \tag{7.6}$$

$$\frac{KC}{R_\theta} = \frac{1}{M_W} P(\theta)^{-1}. \tag{7.7}$$

In the simpler Debye method, intensity measurements are conducted at different concentrations but not at different scattering angles, therefore allowing the determination of M_w and A_2, but not of R_g.[16,17] This method applies to very dilute solutions to avoid multiple scattering.

The scattered intensity depends on the shape and dimension of the particle and is proportional to the sixth power of the particle radius (i.e., squared volume). Thus, particles with higher R_g values result in increased light scattering. R_g is also related to particle shape, although it can be calculated with no prior assumption on shape. Particles with the same M_w but with different shapes differentially scatter the incident light (e.g., light scattering by a globular particle is more intense than scattering by an equivalent particle with a cylindrical shape). For a more detailed description, please refer to **refs.** 16 through **19**. There is no standard solution for calibrating the system. However, using protein solutions of known molecular weight is a good way to calibrate it.

7.2.1. Samples Preparation

Heed the following when preparing samples:

- Minimize dust in the sample.
- Filter all solvents using units with a pore diameter of around 0.02 μm to 0.2 μm.
- Allow prepared solutions to stand for a period that ensures adequate solvation; the period depends on the sample, it may be more than 24 hours or even up to several days.
- Rigorously clean all glassware and apparatus, and ensure they are free from scratches.
- Prepare samples and storage apparatus in a laminar flow cabinet to minimize dust contamination.
- Very small particles, such as proteins, in aqueous solutions often require filtering (the recommended filter is one with small pores) and centrifuging to eliminate residual particles and microscopic bubbles (e.g., 1500 *g* for 30 min).

7.3. Dynamic Light Scattering

DLS is based on scattering fluctuation in a small volume on the time scale of the molecular diffusion (typically microseconds), due to Brownian motion of the particles (arising from the random collision of

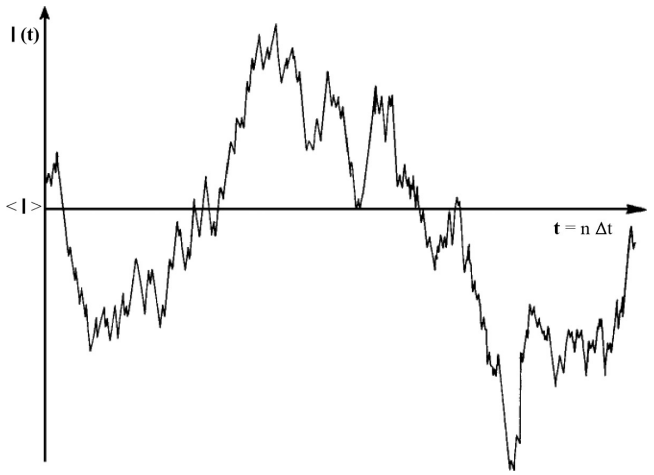

Figure 7.2. Representation of light scattering fluctuations from a small detection volume in the microsecond time range. <I> represents the average scattered intensity.

molecules). This motion allows the light scattered by particles to be shifted according to the Doppler effect. However, for large molecules the velocity is very low and, as a consequence, frequency shifts from Doppler effect are negligible. Hence, it is not possible to obtain the diffusion coefficient from frequency shift analysis. As the molecules diffuse randomly in the illuminated volume of the sample, they tend to randomly cluster and separate. This causes a variation of the scattered light in the local illuminated volume (**Fig. 7.2**). Thus, the diffusion coefficient of the particles can be obtained from an intensity autocorrelation function (**Fig. 7.3**). The decay rate (Γ) of the intensity autocorrelation function is given by the following relation:[2]

$$\Gamma = Dq^2. \tag{7.8}$$

Therefore, the correlation kinetics depend on the intensity-weighted diffusion coefficient (D), which can be calculated using several methods, such as cumulants[20,21] or CONTIN.[22,23] The cumulant method uses a monoexponential correlogram fit to get information about an average D, while CONTIN uses a multiexponential correlogram fit to assess D distribution in a solution (**Fig. 7.4**). Using the Stokes–Einstein equation,

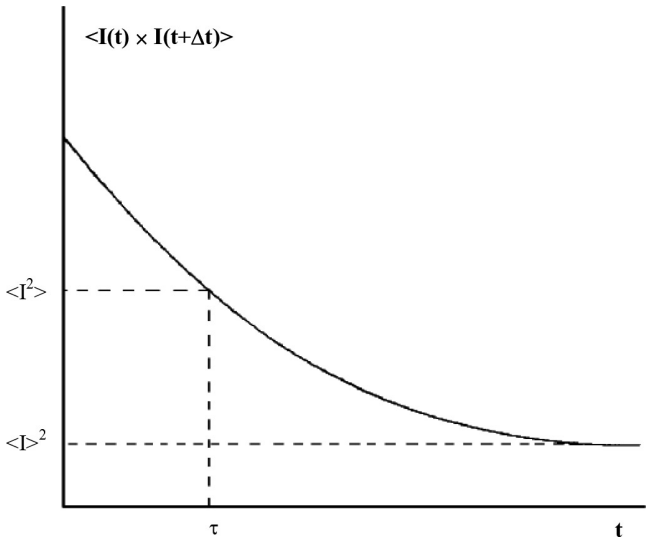

Figure 7.3. Schematic representation of the autocorrelation function. This represents the correlation between scattering intensities with a t interval between them, averaged and represented as a function of t. τ represents the relaxation time at which the correlation function decays to 1/e of its initial value.

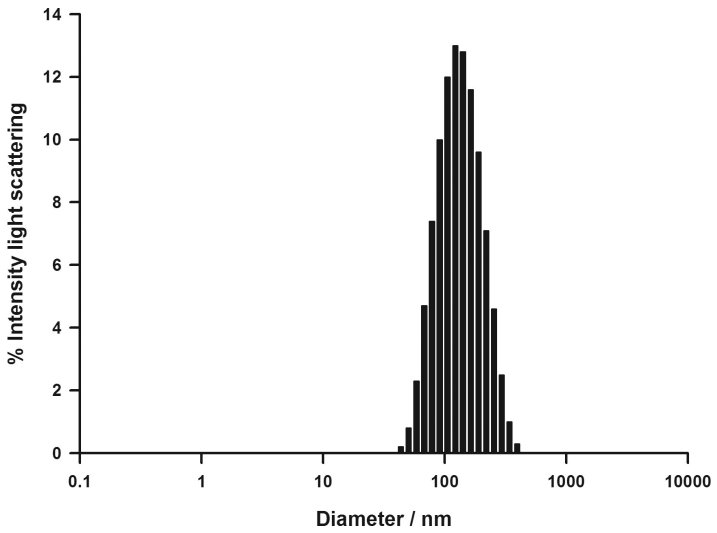

Figure 7.4. Size distribution of phosphatidylcholine (POPC) large unilamellar vesicles in pH 7.4 Tris-HCl buffer, at 37°C, obtained on a Malvern Nano ZS equipment using the CONTIN method.

the value of the hydrodynamic radius (R_H) can be determined from D (for a detailed description see **ref. 2**):

$$D = \frac{\kappa T}{6\pi\eta R_H}, \tag{7.9}$$

where η is the dispersant viscosity, κ the Boltzmann constant, and T the absolute temperature. Depending on equipment and quality of sample preparation, the range of detection of R_H varies from 0.6 nm to 6 μm. To ensure accuracy in measuring particle size, latex beads of different sizes can be used to calibrate the system.

7.3.1. Samples Preparation

Sample contamination by "dust" (a general designation in light-scattering experiments for almost any kind of macrostructure contaminant) can affect measurements and bias results. As the scattered intensity is proportional to the sixth power of the size, only a few macrostructures can prevent study of a sample. Samples should be prepared directly in a clean measurement cell made of plastic, glass, or quartz. When the cells are not disposable, or even when using new cells, the washing process must eliminate dust or other scattering particles that could affect measurements. Remove traces of detergents, lipids, and dust particles from glass or quartz cell inner surfaces by washing for approximately 30 min in dilute chromosulfuric solution (orange colored; made from a concentrate of 40 g sodium or potassium dichromate dissolved in 100 mL water to which 1 to 2 L concentrated sulfuric acid has been added until solution turns brown) or with commercially available Hellmanex® II solution from Hellma. After washing with chromosulfuric solution, cuvettes should be extensively rinsed with ethylenediaminetetraacetic acid (EDTA; 1% weight per volume [w/v], pH 9.5) to remove chromium ions and then with distilled water previously filtered with a 0.2 μm pore filter device. To remove lipid content, rinse cells several times with dichloromethane, ethanol, and distilled water previously filtered with a 0.2-μm-pore filter device. Since most plastic cells cannot with stand organic solvents, they can be used only once and never cleaned. However, filter devices can and should be used to minimize dust

contamination of plastic cells. The samples can be prepared directly in a syringe and filtered though filter devices of different pore sizes. The best filters to use for peptide filtration are those that ensure low protein binding and a minimal loss of peptidic concentration in the sample (e.g., cellulose acetate, polyethersulfone, and polyvinylidene fluoride filters). Sometimes filtration is not sufficient or appropriate to remove dust particles. When this happens use centrifugation to remove larger particles and retain only the supernatant to measure the molecular properties, or even make measurements with the dust particles pelleted at the bottom of the measurement cell. Ultrasonication can also be used to break up some agglomerates in solution. However, depending on the power of the sonication used, this process may contaminate the sample (e.g., with titanium particles) or change its native properties.

7.4. ζ-Potential

Charged particles, such as proteins and peptides, suspended in a solution attract ions of opposite charge to their surface. These ions are strongly bound, forming a layer covering particle surfaces, commonly called the Stern layer (**Fig. 7.5**). Another layer outside the Stern layer also forms where ions diffuse more freely. When particles travel through the solution, the strongly attached ions move with it. In the diffuse boundary the ions do not move with the molecule. The potential that exists at this boundary is called the ζ-potential. This potential is calculated by the electrophoretic mobility of the particles in solution, in the presence of an electric field, to the electrode of opposite charge. Viscous forces oppose movement of the particles until equilibrium, when a constant velocity is reached. Electrophoretic mobility can be calculated by laser Doppler velocimetry in Zetasizer devices, in which particle velocity is related to frequency, measured by intensity fluctuation of the scattered light. Sensitivity of the Doppler effect to the low mobility of larger particles is very low, making it difficult to calculate electrophoretic mobility. Some newer devices can use a different method for calculating electrophoretic mobility. This method was developed in the early 1990s by Miller et al.[24] and is based on phase shift analysis, where differences

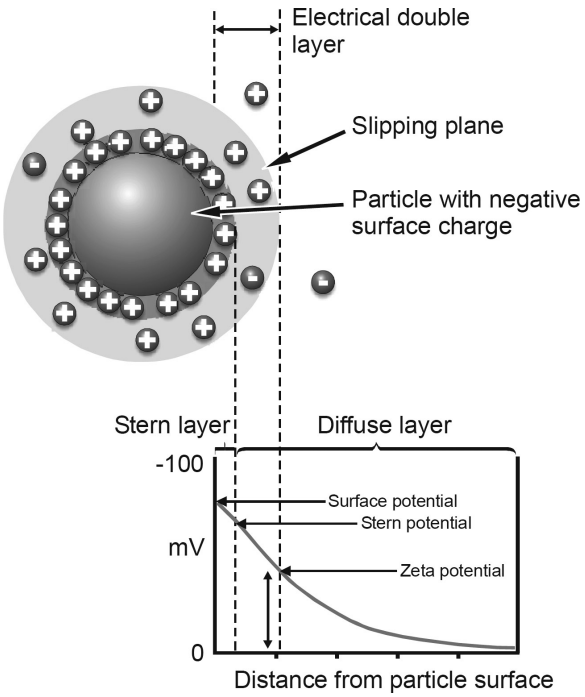

Figure 7.5. Distribution of electrical potential in the double layer region surrounding a charged particle showing the position of the zeta potential.[35]

in phases between the unshifted reference beam and the sample-scattered beam are analyzed with higher sensitivity. This phase shift is related to the position of the particle. Hence, the mean phase change with time yields the electrophoretic motion.[24,25] Using Henry's relation, it is possible to calculate the ζ-potential of the particle (for a more detailed description see **refs. 26** and **27**):

$$U_E = \frac{2\varepsilon z f(ka)}{3\eta}, \qquad (\mathbf{7.10})$$

where z is the ζ-potential, U_E—the electrophoretic mobility, and $f(ka)$—Henry's function. The value of this function is 1.5 when particles are suspended in aqueous solutions (Smoluchowski approximation) and 1 when they are in nonaqueous media (Hückel approximation). The ζ-potential

measurements should be made in a liquid transparent continuous phase, where the dispersed phase has a different refractive index. This method allows accurate ζ-potential measurements for samples with particle sizes larger than 5 nm and smaller than 10 μm. If a horizontal field is applied, the ζ-potential measurements can be carried on while the sample is sedimenting. Samples with known ζ-potential should be used to calibrate and validate the system. The only ζ-potential reference sample that follows the requirements of the National Institute of Standards and Technology (NIST) is Standard Reference Material (SRM) 1980. This sample is a 500 mg/L goethite (α-FeOOH) suspension, saturated with 100 μmol/g phosphate in a 50 mM sodium perchlorate electrolyte solution, at pH 2.5. When prepared according to the procedure supplied by NIST, its electrophoretic mobility is $(2.53 \pm 0.12) \times 10^{-8}$ $m^2/V{\cdot}s$, corresponding to a ζ-potential of 32 ± 1.5 mV, if the Smoluchowski model is used. However, most studied samples are negatively charged, suggesting the use of a standard with also negative charge. Since no negatively charged samples fulfill the requirements of NIST, it is common to use carboxylate-modified polystyrene sulfate latex microspheres (beads) as ζ-potential standard. A standard with these characteristics, produced by Malvern Instruments (Worcestershire, United Kingdom), is dispersed in a pH 9.22 buffer and has a ζ-potential of −50 ± 5 mV.

7.4.1. Samples Preparation

The preparation of samples for ζ-potential measurements is similar to those described above. However, some samples are too concentrated to be directly measured and they require dilution. The dilution process must not change the properties of the particle surface. One way to ensure this is by filtering and centrifuging some clear liquid from the original sample and using that to dilute the stock solution to the desired concentration. This usually maintains the equilibrium between liquid and surface. Sometimes extraction of supernatant is not possible, making it necessary to wait for sample sedimentation before measuring the ζ-potential of the diluted particles left in the supernatant. Another possibility is to dialyze the concentrate sample against a solution with the desired ionic strength. If the particles to be measured are positively charged, avoid storage in glass containers, because dissolution of glass can lead to adsorption of negatively charged species on the particles. For emulsion

systems, dilution is problematic since the phase volume ratio can be changed and, consequently, lead to changes in the surface properties. In successive measurements, the original ζ-potential value may increase. In these circumstances a delay between measurements will allow sample stabilization and subsequent coherent and reliable values.[28] When samples with more than one solute are used, control measurements of each individual solute should always be made. In some situations, these measurements allow establishing a threshold with the software, so as to remove background signal from a free solute that is contributing to ζ-potential values (e.g., discarding the contribution of a peptide that is free in solution when studying peptide–membrane complexes).

7.5. Applications

The methods described above are very useful for studying interaction and behavior of proteins or peptides in solution. Both SLS and DLS can be used for determining crystal growth conditions.[29] Another possible use concerns the process of association or dissociation of proteins induced by several conditions. In the biomedical field, this process can indicate loss of biological activity. More frequent are the applications of SLS, DLS, and ζ-potential measurements in membrane-active-peptide studies. The peptide–membrane interaction often leads to changes in the physical properties of the membrane (e.g., size, charge, and shape). Membrane-active peptides vary in their hydrophobic and charged amino-acid contents. These peptide properties are believed to determine their interaction-related effects on membranes.

ζ-potential measurements are a useful tool to evaluate membrane–peptide interactions. Many biological systems, like bacterial membranes, are composed of a high proportion of negative lipid, which ensures the selectivity and efficient activity of positively charged antibiotics. In addition to negative lipids, endotoxin or lipopolysaccharide (LPS) is present in the outer leaflet of the outer membrane of Gram-negative bacteria, further contributing to an overall negative charge. Because of the high relevance of LPS to human diseases, peptides with positive charge and LPS-binding properties are needed and sought. Antimicrobial peptides, such as those based on *Limulus* antilipopolysaccharide factor,

have LPS-binding properties, reducing their overall charge, as measured by ζ-potential technique.[30] This potential reduction ensures the high affinity of those peptides toward LPS moieties. Using the same approach, Willumeit et al. studied the effect of an α-helical peptide antibiotic, named NK-2, on phospholipid membranes representative of bacterial and human cell cytoplasmic membranes.[31] **Fig. 7.6** shows the effect of the peptide on each membrane. The addition of NK-2 had no influence on the ζ-potential of 1,2-dipalmitoyl-*sn*-glycero-3-phosphatidylcholine (DPPC) membranes. Otherwise, for 1,2-dipalmitoyl-*sn*-glycero-3-phosphoethanolamine (DPPE) and 1,2-dipalmitoyl-*sn*-glycero-3-[phosphor-rac-(1-glycerol)] (DPPG) membranes, charge neutralization was observed. For DPPE membranes the ζ-potential was neutralized at low [peptide]-to-[lipid] molar ratio, which is representative of an electrostatic interaction. At higher [peptide]-to-[lipid] molar ratios there is a charge overcompensation, suggesting a hydrophobic interaction after the saturation of the negative surface charge. For DPPG membranes a stronger overcompensation occurs, corresponding to a higher affinity toward NK-2 for DPPG than for DPPE membranes. These results indicate that the peptide is more selective toward bacterial membranes (considering DPPG membranes as their model system) than to human cell cytoplasmic membrane (DPPC mimetic systems) and interacts with them, adsorbing on and inserting in the membranes.

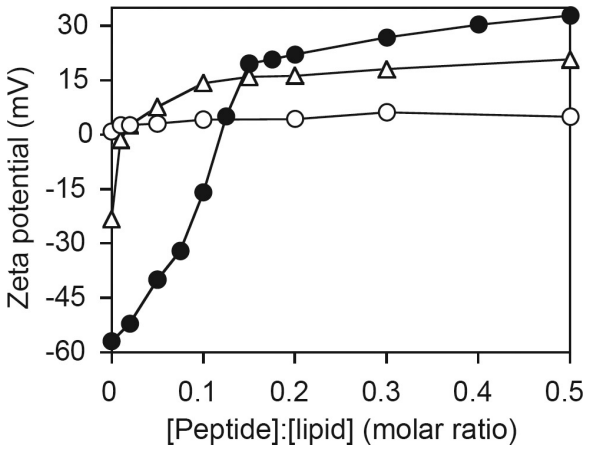

Figure 7.6. Variation of the ζ-potential of phospholipid vesicles of DPPC (open circles), DPPE (open triangles) or DPPG (closed circles) with the [NK-2]/[phospholipid] molar ratio.[31]

Cell-penetrating peptides (CPPs) have been used as vectors for cytoplasmic and nuclear delivery of hydrophobic biomolecules and drugs. The design of new peptides as CPPs is a possible strategy for an alternative therapeutic approach. Their positive charge allows electrostatic interaction with membranes composed of negative lipid and enables ζ-potential measurements to study that effect. **Fig. 7.7** shows results of a ζ-potential study of the interaction of poly-L-arginine, a positively charged peptide, with lipid vesicles.[13] This peptide is believed to be a good system for facilitating transport of drugs through biological membranes. As shown in **Fig. 7.7**, ζ-potential measurements (at different temperatures) of the addition of peptides to mixed lipid vesicles consisting of 1-palmitoyl-2-oleoyl-*sn*-glycerol-3-phosphatidylcholine, cholesterol, and dihexadecylphosphate (POPC–Chol–DHP) results in less negative ζ-potential values. This is due to adsorption of the peptide to the membrane. However, at 65°C, where lipids are in the liquid-crystalline phase, the plateau is reached at higher molar ratios of the guanidinium group of the peptide relative to the phosphate group of the lipid membrane. This could be due to partial incorporation of the peptide, which results in a hydrophobic interaction instead of surface adsorption. As this happens the phosphate groups of the lipid are exposed and interact more

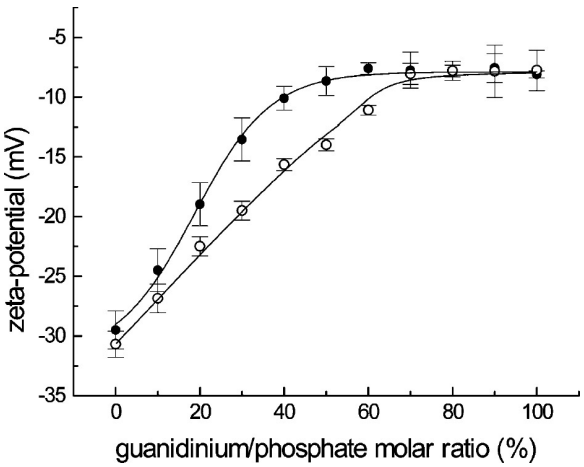

Figure 7.7. ζ-potential of POPC–Chol–DHP lipid vesicles as a function of guanidium/phosphate molar ratios, before (closed symbols) and after (open symbols) incubation at 65°C with polyarginine.13 Reproduced with permission of the American Chemical Society.

freely with other peptide molecules. These studies have found that before phase transition of the lipids the peptide is mainly adsorbed and after phase transition the peptide inserts in the membrane, leading to drug transport across the membrane. In the same way, Yaroslov et al. studied polylysine, a positive polypeptide, and showed that it can interact with lipid vesicles composed of negative lipids (in this case cardiolipin), resulting in a slightly positive complex.[32] This interaction with negative lipid enables increase in permeation of vesicles of doxorubicin (or dox, a fluorescent antitumor drug) when lipid vesicle charge is close to zero, corresponding to peptide being electrostatically adsorbed to the negative lipid.

Almost all the cationic peptides induce aggregation of negatively charged lipid vesicles at high enough peptide concentrations. Besides this, many hydrophobic peptides are capable of interacting with neutral-charge lipids and inducing their aggregation. These properties can help the design of new peptides with antibiotic action. Using DLS, Vagt et al. studied the effect of structure on the biological activity of three variants of coiled-coil peptides.[14] **Fig. 7.8** shows the strongest effect on variant 1 peptide, while the basis peptide has no interaction. This higher effect on variant 1, on membrane composed of negative charge, over other variant

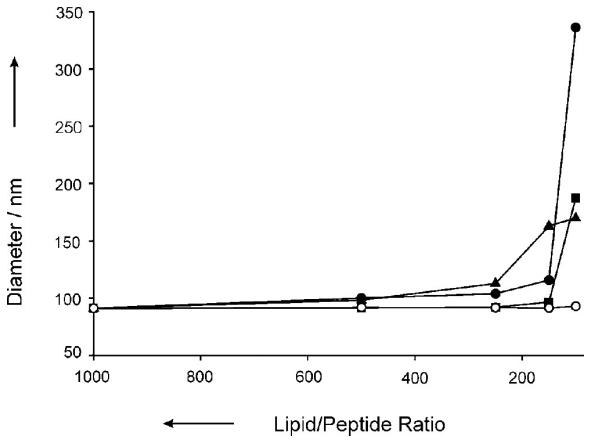

Figure 7.8. Hydrodynamic diameter of POPC:POPG (1:1) large unilamellar vesicles at different lipid/peptide ratios: basis peptide (open circles), variant 1 (closed circles), variant 2 (closed squares) and variant 3 (closed triangles).[14] Reproduced with permission of Wiley-VCH Verlag GmbH & Co. KGaA.

peptides and the basis peptide has to do with variant 1's secondary structure and with its charge as well. Although the variant 1 and the basis peptides both retain a stable α-helical coiled coil, variant 1 has an overall positive charge and the basis peptide has a neutral charge. The other variant peptides have an overall positive charge but also higher repulsive forces on their secondary structures, which result in an unstable α-helical coiled-coil conformation. The results show that a positive charge and a stable α-helical folding are characteristics that promote a stronger effect on vesicle aggregation. Cummings et al. observed by DLS the size increase of 1-palmitoyl-2-oleoyl-*sn*-glycerol-3-phosphatidylglycerol (POPG) vesicle aggregates upon addition of cryptdin-4, an antimicrobial peptide found in mice that causes aggregation and hemifusion of negative lipid vesicles.[33] The lipid vesicles' aggregation in the presence of cryptdin-4 reaches a limit for very large aggregates, less prone to fusion. Thus, the ability of cryptdin-4 to promote stable fusion of anionic lipid vesicles can create vesicular structures that may be used as drug delivery agents. Herbig et al. used several techniques, including DLS, to evaluate whether a vascular endothelial cadherin-derived CPP (pVEC) and W2-pVEC were able to affect biomembrane integrity.[9] W2-pVEC is a peptide derived from pVEC with the substitution of an isoleucine for a tryptophan. Although integrity of the DPPC large unilamellar vesicles (LUVs) is not impaired at low peptide concentrations, it remained unclear whether at higher peptide concentrations this integrity is compromised. DLS studies at 25°C (**Fig. 7.9**) show a small increase of membrane vesicle diameter with the addition of the peptides. This increase is more pronounced for W2-pVEC addition. To find whether this increase was a consequence of peptide insertion in or association on the membrane vesicles or due to membrane vesicle damage, the authors monitored the polydispersity indices of the size distribution. As none of the peptides caused significant increase in the polydispersity index, it was concluded that the increase in vesicle diameter was due to peptide insertion. If the integrity of the membrane vesicles had been affected, a significant change in the polydispersity index values would have been expected, as a consequence of the formation of larger and smaller membrane vesicles or to membrane vesicle aggregation. At 50°C, with DPPC LUVs in the fluid phase (**Fig. 7.9**), addition of the peptides causes an initial higher membrane vesicle diameter, which decreases over time. Analysis of the polydispersity index values indicated that at the very first moment of pVEC addition significant increase of the polydispersity index also

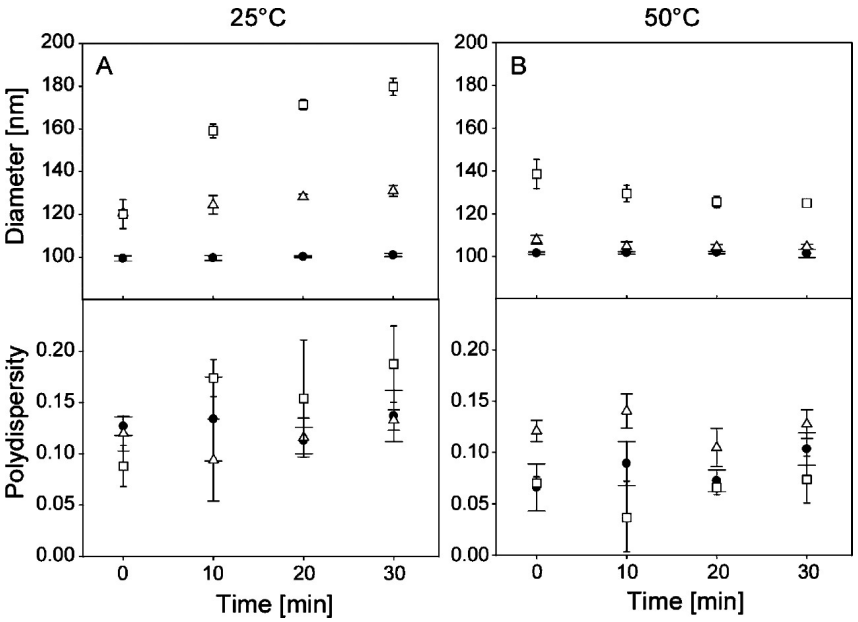

Figure 7.9. Diameters and polydispersity indexes of DPPC large unilamellar vesicles without and with peptide, monitored over 30 min. DPPC LUV alone (closed circles) were compared with LUV in the presence of the peptides pVEC (open triangles) or W2-pVEC (open squares).[8]

occurs, which is lost over time. This variation of the polydispersity index was not seen for W2-pVEC. The results show that the interaction of both peptides with the membrane vesicle is followed by insertion, without damage of the membrane vesicle structure.

The fusion process of lipid vesicles in the presence of peptides can also be evaluated by SLS. Intensity measurements for vesicle dispersions at different pH in the presence of wtfp (wild type fusion peptide of hemagglutinin) and mutfp (sequence of the fusion peptide of hemagglutinin with a mutation at the N-terminal glycine residue) are shown in **Fig. 7.10**.[34] The average M_w of the scattering particles for wtfp at neutral pH (1.1×10^7 g · mol^{-1}) is lower than that obtained at acidic pH (3.5×10^7 g · mol^{-1}). In the presence of mutfp there was no difference in the average M_w calculated at neutral and acidic pH (1.2×10^7 g · mol^{-1}). Trivedi et al. showed by this methodology that wtfp has more effect on vesicular fusion than mutfp and, consequently, the important role of the N-terminal in fusion activity.

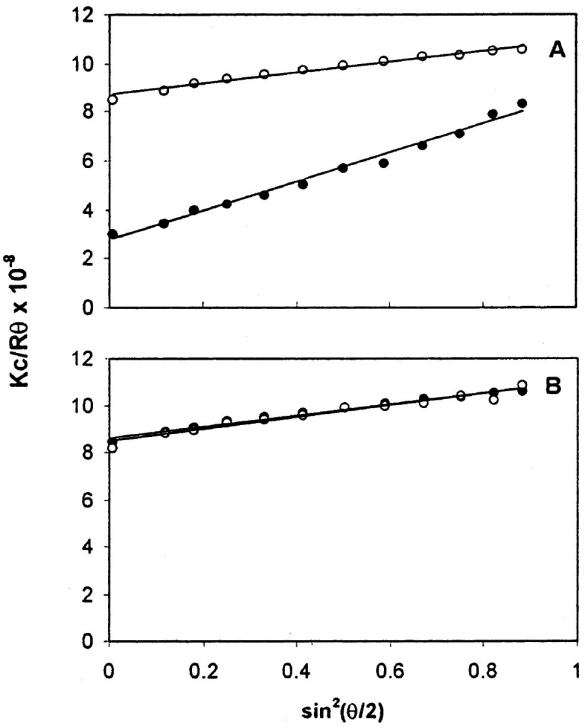

Figure 7.10. Determination of the average molecular weight, by SLS, for vesicular dispersion in the presence of fusion peptides wtfp (A) and mutfp (B), at acidic (closed symbols) and neutral pH (open symbols).[34] Reproduced with permission from Elsevier.

7.6. Other Practical Aspects

Independently of the application, some practical conditions must be fulfilled in light-scattering experiments. The light source must be monochromatic and continuous, in order to have a signal of the same frequency. Lasers are the only practical source of radiation that match these conditions. Another requirement to do light-scattering experiments is related to stray light. It can be very problematic, since uncontrolled light can mix with the light from the scattering volume and generate false signals.[19] As mentioned above, the contamination by dust and other large particles can also be a severe problem since scattering intensity depends on the sixth

power of the radius of the particle. Even with a careful sample preparation process, the addition of filtration or centrifugation, or both, can be useful for eliminating contamination.[16] Absorbing samples are a limitation to light-scattering measurements since efficiency of the autocorrelation can be considerably reduced.[19] Loss of signal is the major consequence of this limitation, since there is attenuation of the incident and scattered light. Increasing the power of incident light is not recommended, since heating problems may cause alterations in the diffusion coefficient. Fluorescent samples can also interfere with the measurement. A highly fluorescent sample, with absorption at the wavelength of the laser used for the light-scattering measurements, can be impossible to characterize by these methodologies. On ζ-potential measurements, changes in the pH should be avoided because of alterations in protonation of the peptide amino acid residues. Ionic strength should be kept low (not significantly above the physiologic saline concentration), as high conductivity causes Joule heating of the sample and affects the particle mobility as well as its integrity.[26,27] However, a too low conductivity would also impair the electrophoretic mobility. A minimal salt concentration (e.g., NaCl 0.1 mM) is needed for field stability and double layer definition.[27]

7.7. Conclusion

Peptides constituted by charged residues and an amphipathic structure can have a strong interaction with membranes. This interaction can be studied by spectroscopic techniques without affecting the system. The interaction of peptides with membranes may be accompanied by membrane changes, such as aggregation or physical damage, which can be measured by their size and scattering intensity using DLS or SLS techniques. Charged residues in peptide structure can promote electrostatic interaction with membranes and lead to variation of their surface charge. This membrane surface-charge alteration in the presence of peptides can be efficiently followed by ζ-potential measurements. Together, these methods can contribute to the determination of mechanisms of action of membrane-active peptides at the molecular level, as well as to the identification of new peptides with higher pharmaceutical activity.

Acknowledgments

This work was partially supported by the Fundação para a Ciência e Tecnologia (FCT) of the Portuguese Ministry of Science, Technology and Higher Education. M.M.D. acknowledges the grant SFRH/BD/41750/2007 from FCT.

References

1. Strutt J. **On the scattering of light by small particles.** *Phil Mag* 1871, **41**:447–454.
2. Berne BJ and Pecora R. ***Dynamic Light Scattering - with Application to Chemistry, Biology and Physics.*** Malabar, Florida: Robert E. Krieger Publishing, 1990, pp. 1–23.
3. Santos NC and Castanho MA. **Teaching light scattering spectroscopy: The dimension and shape of tobacco mosaic virus.** *Biophys J* 1996, **71**(3):1641–1650.
4. Zimm BH. **Apparatus and methods for measurement and interpretation of the angular variation of light scattering - Preliminary results on polystyrene solutions.** *J ChemPhys* 1948, **16**(12):1099–1116.
5. Zimm BH. **The scattering of light and the radial distribution function of high polymer solutions.** *J Chem Phys* 1948, **16**(12):1093–1099.
6. Bohidar HB. **Light scattering and viscosity study of heat aggregation of insulin.** *Biopolymers* 1998, **45**(1):1–8.
7. Bridelli MG. **Self-assembly of melanin studied by laser light scattering.** *Biophys Chem* 1998, **73**(3):227–239.
8. Matsunami H, Fujita C, Ogawa K, and Kokufuta E. **Static light scattering study of complex formation between protein and neutral water-soluble polymer.** *Colloids Surf B* 2007, **56**(1–2):149–154.
9. Herbig ME, Assi F, Textor M, and Merkle HP. **The cell penetrating peptides pVEC and W2-pVEC induce transformation of gel phase domains in phospholipid bilayers without affecting their integrity.** *Biochemistry* 2006, **45**(11):3598–3609.
10. Panyukov Y, Yudin I, Drachev V, Dobrov E, and Kurganov B. **The study of amorphous aggregation of tobacco mosaic virus coat protein by dynamic light scattering.** *Biophys Chem* 2007, **127**(1–2):9–18.

11. Papish AL, Tari LW, and Vogel HJ. **Dynamic light scattering study of calmodulin-target peptide complexes.** *Biophys J* 2002, **83**(3):1455–1464.

12. Reichert J, Grasnick D, Afonin S, Buerck J, Wadhwani P, and Ulrich AS. **A critical evaluation of the conformational requirements of fusogenic peptides in membranes.** *Eur Biophys J* 2007, **36**(4–5):405–413.

13. Tsogas I, Tsiourvas D, Nounesis G, and Paleos CM. **Interaction of poly-L-arginine with dihexadecyl phosphate/phosphatidylcholine liposomes.** *Langmuir* 2005, **21**(13):5997–6001.

14. Vagt T, Zschornig O, Huster D, and Koksch B. **Membrane binding and structure of de novo designed alpha-helical cationic coiled-coil-forming peptides.** *Chemphyschem* 2006, **7**(6):1361–1371.

15. Volodkin D, Ball V, Schaaf P, Voegel JC, and Mohwald H. **Complexation of phosphocholine liposomes with polylysine. Stabilization by surface coverage versus aggregation.** *Biochim Biophys Acta* 2007, **1768**(2):280–290.

16. Brown W. ***Light Scattering—Principles and Development.*** Oxford: Clarendon Press, 1996, pp. 1–27.

17. Chu B. ***Laser Light Scattering—Basic Principles and Practice.*** New York: Academic Press, 1991, pp. 13–20.

18. Harding SE, Satelle DB, and Bloomfield VA. ***Laser Light Scattering in Biochemistry.*** Cambridge: The Royal Society of Chemistry, 1972, pp. 3–22.

19. Johnson CS and Gabriel DA. ***Laser Light Scattering.*** New York: Dover Publication. 1994, pp. 3–7.

20. Frisken BJ. **Revisiting the method of cumulants for the analysis of dynamic light-scattering data.** *Appl Opt* 2001, **40**(24):4087–4091.

21. Koppel DE. **Analysis of macromolecular polidispersity in intensity correlation spectroscopy: The method of cumulants.** *J Chem Phys* 1972, **57**(12):4814–4820.

22. Provencher SW. **A constrained regularization method for inverting data represented by linear algebraic or integral-equations.** *Comput Phys Commun* 1982, **27**(3):213–227.

23. Provencher SW. **CONTIN: A general purpose constrained regularization program for inverting noisy linear algebraic and integral equations.** *Comput Phys Commun* 1982, **27**(3):229–242.

24. Miller JF, Schatzel K, and Vincent B. **The determination of very small electrophoretic mobilities in polar and nonpolar colloidal dispersions using phase-analysis light-scattering.** *J. Colloid Interface Sci* 1991, **143**(2):532–554.

25. Tscharnuter WW. **Mobility measurements by phase analysis.** *Appl Opt* 2001, **40**(24):3995–4003.

26. Kirby BJ and Hasselbrink EF. **Zeta potential of microfluidic substrates: 1. Theory, experimental techniques, and effects on separations.** *Electrophoresis* 2004, **25**(2):187–202.

27. Delgado AV, Gonzalez-Caballero F, Hunter RJ, Koopal LK, and Lyklema J. **Measurement and interpretation of electrokinetic phenomena.** *J Colloid Interface Sci* 2007, **309**(2):194–224.

28. Kaufman ED, Belyea J, Johnson MC, Nicholson ZM, Ricks JL, Shah PK, Bayless M, Pettersson T, Feldoto Z, Blomberg E, Claesson P, and Franzen S. **Probing protein adsorption onto mercaptoundecanoic acid stabilized gold nanoparticles and surfaces by quartz crystal microbalance and zeta-potential measurements.** *Langmuir* 2007, **23**(11):6053–6062.

29. Wilson WW. **Light scattering as a diagnostic for protein crystal growth—A practical approach.** *J Struct Biol* 2003, **142**(1):56–65.

30. Andra J, Lamata M, Martinez de Tejada G, Bartels R, Koch MH, Brandenburg K. **Cyclic antimicrobial peptides based on Limulus anti-lipopolysaccharide factor for neutralization of lipopolysaccharide.** *Biochem Pharmacol* 2004, **68**(7): 1297–1307.

31. Willumeit R, Kumpugdee M, Funari SS, Lohner K, Navas BP, Brandenburg K, Linser S, and Andra J. **Structural rearrangement of model membranes by the peptide antibiotic NK-2.** *Biochim Biophys Acta* 2005, **1669**(2):125–134.

32. Yaroslavov AA, Kuchenkova OY, Okuneva IB, Melik-Nubarov NS, Kozlova NO, Lobyshev VI, Menger FM, and Kabanov VA. **Effect of polylysine on transformations and permeability of negative vesicular membranes.** *Biochim Biophys Acta* 2003, **1611**(1–2):44–54.

33. Cummings JE and Vanderlick TK. **Aggregation and hemi-fusion of anionic vesicles induced by the antimicrobial peptide cryptdin-4.** *Biochim Biophys Acta* 2007, **1768**(7):1796–1804.

34. Trivedi VD, Yu C, Veeramuthu B, Francis S, and Chang DK. **Fusion induced aggregation of model vesicles studied by dynamic and static light scattering.** *Chem Phys Lipids* 2000, **107**(1):99–106.

35. ***Zetasizer Nano User Manual.*** Malvern, Worcestershire, United Kingdom: Malvern Instruments Ltd., 2007:252.